

## THE DYNAMICS OF VORTICES IN VERTICAL SHEAR FLOWS

By Roger K. Smith<sup>1\*</sup> and Wolfgang Ulrich<sup>1</sup>  
and  
Graeme Sneddon<sup>2</sup>

<sup>1</sup>*Meteorological Institute, University of Munich*

<sup>2</sup>*Mathematics Department, James Cook University, Townsville, Australia*

04 May 2000

### SUMMARY

A simple two-layer analogue model is used to elucidate aspects of vortex motion in a vertically-sheared zonal flow. The model is based on the idea that a vortex can be considered as the sum of a pair of barotropic vortices, one whose vorticity, or potential vorticity, resides in the upper layer and the other resides in the lower layer. Each vortex has an associated tangential velocity distribution in the other layer, which advects the vortex in that layer. The strength of this velocity distribution is characterized by a coupling parameter, which, in the case of quasi-geostrophic vortices, is related to the Rossby depth scale. Besides their mutual advection, the component vortices are differentially advected by vertical shear. The model leads to a set of coupled ordinary differential equations for the motion of each component vortex, which may be solved analytically in certain circumstances. The calculations indicate two types of flow behaviour according to the strength of the component vortices, the degree of vertical coupling and the strength of the shear. For weak shear and/or strong vortices and strong coupling, the vortices rotate around each other as their mean centre translates with a fraction of the mean zonal flow. For strong shear and/or weak vortices and weak coupling, the vortices undergo a partial rotation while they are in proximity, but become progressively separated by the shear. The calculations are an aid to understanding the range of behaviour of vortices in shear in numerical calculations by other authors and it is reasonable to presume that the processes represented by the model are fundamental processes in tropical cyclones also.

The analogue model is evaluated in the context of quasi-geostrophic theory, where the breakdown into the component vortices can be accomplished and where the complete problem can be solved numerically without approximation. The results of the quasi-geostrophic model are contrasted with those of other recent studies of baroclinic vortices in the absence of vertical shear.

KEYWORDS: Vortex dynamics Two-layer shear flow Tropical cyclones Hurricanes

### 1. INTRODUCTION

In recent years there has been a number of numerical modelling studies of vortex motion in a vertically-sheared environmental flow directed towards understanding aspects of hurricane motion. The basic thought experiment considers the subsequent motion of an initially-symmetric and upright vortex when subjected to uniform shear on an  $f$ -plane or on a beta-plane. A variety of models has been used (e.g. two-layer, multi-level), some of them dry (Wu and Emanuel, 1993; Wang *et al.*, 1993; Jones, 1995, 2000a,b; Dengler and Reeder, 1996; Wang and Holland, 1996) and others including a representation of moist processes (Flatau *et al.*, 1994; Shapiro, 1992; Dengler and Reeder, 1996). Some of the dry models begin with a barotropic vortex (e.g. Jones, 1995; 1999a) while others begin with a baroclinic vortex whose strength decreases with height (e.g. Dengler and Reeder, 1996, Jones, 2000b). Not surprisingly, a range of behaviour has been reported depending on the particular model formulation and on the particular choice of parameters. For example, Madala and Piacsek (1975) showed that under the influence of easterly shear, a vortex on a beta plane has a more polewards track than in the corresponding calculation for a quiescent environment. An additional component of motion to the right of the shear was found also in calculations by Shapiro (1992) and Wang *et al.* (1993). In contrast, in

\* Corresponding author: Meteorological Institute, University of Munich, Theresienstr. 37, 80333 Munich, Germany

the calculations by Wu and Emanuel (1993) and Flatau *et al.* (1994), vortex motion is to the left of the shear vector. A succinct review of the earlier papers is given by Jones (1995) who reconciles the differences in the foregoing calculations and elucidates various mechanisms that are important.

In some of the calculations (e. g. those of Shapiro, 1992, and Flatau *et al.*, 1994) the vortex motion is influenced strongly by the presence of a meridional gradient of potential vorticity (PV), the sign of which depends on the curvature of the shear profile. The advection of PV by the tangential circulation of the vortex gives rise to an azimuthal wave number one PV-asymmetry, which has an associated flow component across the vortex centre in a direction related to that of the ambient PV-gradient. This cross-vortex flow component contributes to the vortex motion as in the case of a barotropic vortex (see e.g. Smith, 1993).

Another mechanism elucidated by Jones *op. cit.*, which appears to account for the vortex motion in the f-plane calculations she carried out, is associated with the vortex tilt produced by the shear. Again the flow evolution may be interpreted using PV-thinking (Hoskins *et al.*, 1985). Initially, the vortex, either barotropic or baroclinic, is tilted in the plane of the shear following which the upper- and lower-vortex centres begin to rotate about each other. This mutual rotation can be understood in terms of upper- and lower PV anomalies associated with the tilted vortex which are displaced in the horizontal relative to each other. The flow associated with the vertical projection of each anomaly advects the other anomaly. The strength of this mutual rotation of the upper and lower vortex centres increases as the penetration depth of the anomalies increases. In geostrophic vortices, the penetration depth is proportional to the length scale of the anomaly, the Coriolis parameter and inversely proportional to the static stability, whereas for stronger vortices it increases as the local inertial stability increases rather than the Coriolis parameter alone (Shapiro and Montgomery, 1993). A similar mechanism was explored by Wu and Emanuel (1993) in a two-layer quasi-geostrophic model in which a hurricane is represented by a point source of mass and zero-PV air in the upper layer, co-located with a point cyclone in the lower layer. In the presence of vertical shear, a plume of zero-PV air streams away from the cyclone. The plume is distorted by the circulation induced by the cyclone in the upper layer, while the cyclone is advected by the flow induced by the plume in the lower layer. In this case the differential advection of the lower cyclonic vortex and the upper anticyclonic plume it produces account for the motion of the cyclone to the left of the shear, whereas, in the calculations for a cyclonic vortex only by Jones *op. cit.*, the differential advection accounts for the motion of the lower vortex to the right of the shear. Flatau *et al.* (1994) attribute the motion to the left of the vertical shear in their calculations to this mechanism.

Some authors explore mechanisms by which vortices can resist the effects of vertical shear. Flatau *et al.* (1994) and Wang and Li (1992) suggest the vertical circulation induced by the tilt can help the vortex to remain vertically coupled, but they do not explain how this coupling arises, while Wang *et al.* (1993) argue that the circulation is such as to oppose the tilting effect of the shear. Jones *op. cit.* shows that while the circulation opposes the tilt at early times, the situation is complicated because the plane of the tilt rotates as the upper- and lower vortex centres rotate about each other. Moreover, the vertical circulation depends on the direction of tilt, not on the direction of the shear. As a result, after a period of time the upper vortex centre lies upshear of the lower centre whereafter the shear contributes to a period of vertical re-alignment of the vortex.

The present paper seeks to isolate the tilting mechanism described by Jones (1995), which appears to explain much of the behaviour in the various models. To elucidate this mechanism further we formulate an analogue system of equations based on a sim-

ple model for a pair of interacting line vortices, or a pair of axi-symmetric distributed vortices, the upper one situated in a uniform flow and the lower one in an environment at rest. In the model, described in section 2, the two vortices are artificially coupled by assuming that the upper vortex has a component of velocity at its centre equal to some fraction  $\alpha$  of the velocity associated with the lower vortex and vice versa. The case of vortices with a radial distribution of vorticity is considered in section 3, where the idealization is made that the vortices are not permitted to distort each other. We show that many features of the behaviour of vortices in vertical shear may be understood in terms of this model. In section 4, calculations are presented for the case of a sheared vortex in a quasi-geostrophic model where the interaction parameter  $\alpha$  and the full structure of the component vortices, including the displacement of the interface between them, can be determined. Detailed comparisons are made between the predictions of the analogue model for this case and the full numerical solution of the problem. Finally, in section 5, we contrast the quasi-geostrophic calculations to previous ones that address the dynamics of baroclinic vortices without vertical shear.

## 2. AN ANALOGUE MODEL

To understand the subsequent motion of a vortex in a vertically-sheared environment, we formulate the following thought experiment illustrated in Fig. 1. Consider two coupled

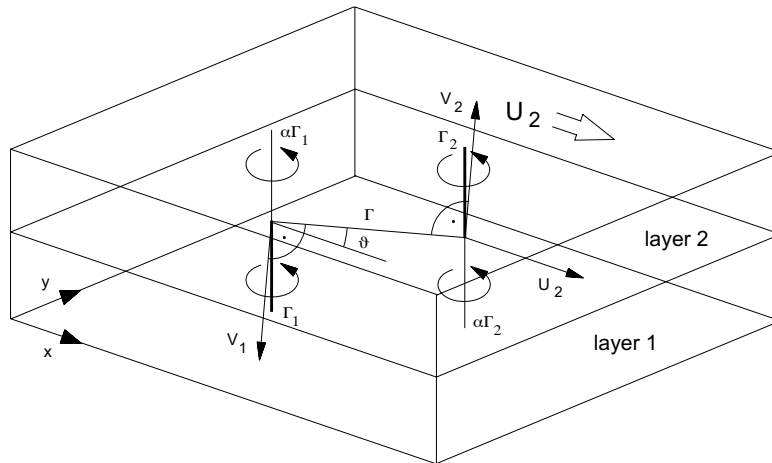


Figure 1. Flow configuration in the analogue model for vortex motion in vertical shear in a two-layer model. The thick solid lines represent line vortices of circulation strength  $2\pi\Gamma_n$  in layer- $n$  ( $n = 1,2$ ) with a projection of strength  $2\pi\alpha\Gamma_n$  in the other layer, indicated by a thinner extension. A uniform zonal flow  $U_2$  in layer-2 advects the upper vortex (vortex-2) to the east. In addition, this vortex has a component of motion  $\mathbf{V}_2$  at right angles to the line joining the two vortices, a result of the flow at its centre associated with vortex-1 in the upper layer. There is no basic flow in the lower layer and vortex-1 translates with velocity  $\mathbf{V}_1$  associated with the flow of vortex-2 in layer-1.

barotropic flows, one of them lying on top of the other. Suppose that the upper flow consists of a point vortex with circulation  $2\pi\Gamma_2$  in an otherwise uniform stream with speed  $U_2$ , while the lower flow consists only of a point vortex with circulation  $2\pi\Gamma_1$ . We

imagine the vortices to be coupled in such a way that the upper vortex has a component of motion equal to a fraction  $\alpha$  of the velocity of the lower vortex at its location, and *vice versa*. The idea would be that the two vortices are initially co-located (or at least close together, but become separated because of the basic state velocity difference  $U_2$  between the layers. As a result, each is influenced to a degree by the rotation field of the other vortex, and this affects their subsequent motion. In this section we present an analytic theory for the motion.

The foregoing model is a thought experiment, or analogue model, because, with the chosen coupling, the vorticity of the upper (lower) vortex would be singular in the lower (upper) layer. The implied singularities in the other layer are conceived as a fundamental part of the vortex and are not allowed to become detached from the parent vortex by the relative motion between the layers. This assumption is not as unrealistic as it might first seem and is in line with the idea that, in a more complete theory, a potential vorticity anomaly in one layer has an intrinsic flow signature in the other layer that moves with it (see e.g. Hoskins *et al.*, 1985, section 4). We return to this point in section 4, where a more complete theory is presented for quasi-geostrophic vortices.

Let the vortices be located at the positions  $\mathbf{x}_1 = (x_1, y_1)$  and  $\mathbf{x}_2 = (x_2, y_2)$  at time  $t$  and let their velocities at that time be  $(u_1, v_1)$  and  $(u_2, v_2)$ . Then their motion is governed by the four coupled ordinary differential equations:

$$(u_1, v_1) = \frac{d}{dt} (x_1, y_1) = \alpha \frac{\Gamma_2}{r} (\sin \theta, -\cos \theta), \quad (1)$$

$$(u_2, v_2) = \frac{d}{dt} (x_2, y_2) = (U_2, 0) + \alpha \frac{\Gamma_1}{r} (-\sin \theta, \cos \theta) \quad (2)$$

where  $r = |\mathbf{x}_2 - \mathbf{x}_1|$  is the horizontal separation distance between them and  $\theta$  is the angle between the line from vortex-1 to vortex-2 and the positive x-axis (see Fig. 1). Setting  $X = x_2 - x_1$  and  $Y = y_2 - y_1$  and noting that  $\cos \theta = (x_2 - x_1) / r$  and  $\sin \theta = (y_2 - y_1) / r$ , Eqs. (1) and (2) become:

$$\frac{d}{dt} (x_1, y_1) = \alpha \frac{\Gamma_2}{r^2} (Y, -X), \quad (3)$$

$$\frac{d}{dt} (x_2, y_2) = (U_2, 0) + \alpha \frac{\Gamma_1}{r^2} (-Y, X), \quad (4)$$

It will be seen that  $\alpha$  is not really necessary: it could be absorbed into the definitions of  $\Gamma_1$  and  $\Gamma_2$ . However, it will be convenient to retain it as a measure of the vertical coupling between the two vortices. Given the initial values of  $x_1, y_1, x_2, y_2$ , Eqs. (3) and (4) can be integrated forward in time using standard techniques (*e.g.* a Runge-Kutta algorithm). However, because a point vortex is singular at its centre, we cannot allow the vortices to be co-located initially, otherwise the equations would be singular when  $r = 0$ . This difficulty is circumvented in section 4 by using vortices with a continuous vorticity distribution. Define  $\bar{x} = (\Gamma_1 x_1 + \Gamma_2 x_2) / (\Gamma_1 + \Gamma_2)$ ,  $\bar{y} = (\Gamma_1 y_1 + \Gamma_2 y_2) / (\Gamma_1 + \Gamma_2)$ , to be the weighted-mean position of the two vortices, or vorticity centroid. Then adding appropriate multiples of the x- and y-components of (3) and (4) gives

$$\frac{d}{dt} (\bar{x}, \bar{y}) = \left[ \left( \frac{\Gamma_2}{\Gamma_1 + \Gamma_2} \right) U_2, 0 \right], \quad (5)$$

Thus the weighted-mean position moves with a uniform speed  $[\Gamma_2 / (\Gamma_1 + \Gamma_2)] U_2$  in the x-direction. In particular, for vortices of equal strength, the mean position moves with a

uniform speed  $\frac{1}{2}U_2$ . Subtracting the components of (3) from the corresponding ones of (4), gives

$$\frac{dX}{dt} = U_2 - \frac{A}{r^2}Y, \tag{6}$$

and

$$\frac{dY}{dt} = \frac{A}{r^2}X, \tag{7}$$

where  $A = \alpha (\Gamma_1 + \Gamma_2)$  is a constant and  $r^2 = X^2 + Y^2$ . Equations 6 and 7 characterize the motion of vortex-2 relative to vortex-1. Upon division, these equations reduce to the single nonlinear ordinary differential equation

$$\frac{dY}{dX} = \frac{X}{\mu (X^2 + Y^2) - Y}, \tag{8}$$

where

$$\mu = \frac{U_2}{A} = \frac{U_2}{\alpha (\Gamma_2 + \Gamma_1)}. \tag{9}$$

With the substitution  $w = X^2$ , Eq. (8) reduces to the linear equation

$$\frac{dw}{dY} - 2\mu w = 2Y (\mu Y - 1), \tag{10}$$

which has the solution:

$$X^2 + Y^2 = ce^{2\mu Y}, \tag{11}$$

where  $c$  is a constant. Possible trajectories of the upper vortex relative to the lower one,  $(X, Y)$ , are shown in Fig. 2. In the discussion that follows we refer to the X-direction as east and the Y-direction as north. Of interest is the 'critical curve' that passes through

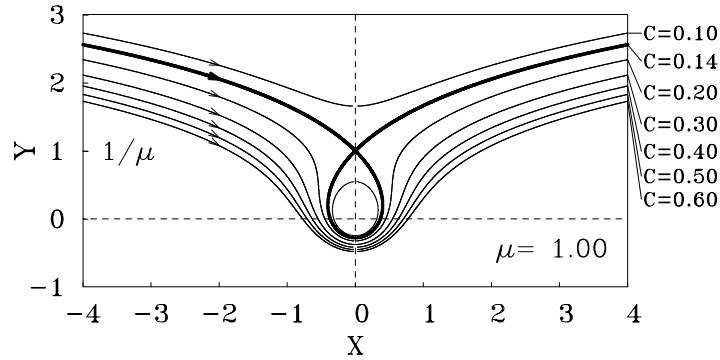


Figure 2. Trajectories  $(X(t), Y(t))$  of the upper vortex relative to the lower one for different initial positions. The critical curve is marked in bold. The axes have been scaled by  $1/\mu$  so that the critical point is at  $(0,1)$ . See text for discussion.

the critical point  $(0,1/\mu)$  of the equation, namely  $X^2 + Y^2 = \mu^{-2}e^{2(\mu Y-1)}$ . The axes in the figure have been scaled by  $1/\mu$  so that the critical point is at  $(0,1)$ . The phase space can be divided into three regions delineated by the critical curve: one where the upper

vortex approaches the lower vortex from the west, passes to the south of it, south of the critical curve, and continues moving to the east after the encounter; another where the upper vortex passes to the north of the lower vortex, north of the critical curve, before continuing on to the east; and a bounded region enclosed by the critical curve in which the relative trajectories are closed loops and the two vortices rotate around each other. In the first case the upper vortex is accelerated by the circulation of the lower one during their encounter, while in the second case it is decelerated. The fact that the two differential equations, (6) and (7), are singular at the origin means that there is not necessarily a critical point inside these loops. Which region the trajectory is in will depend on the starting positions of the two vortices. In summary, the motion of the two-vortex system is composed of a rotation of each about the mean position  $(\bar{x}(t), 0)$ , which translates at speed  $[\Gamma_2 / (\Gamma_1 + \Gamma_2)] U_2$  in the x-direction. Whether or not complete rotations are performed depends on the initial position of the vortices. If they are sufficiently close initially they will rotate around each other. The linear scale of the region enclosed by the critical curve in  $(X, Y)$  space is proportional to  $1/\mu$ . Therefore, 'sufficiently close' depends on the magnitude of this quantity, which is proportional to the average vortex strength, the magnitude of the coupling parameter  $\alpha$ , and inversely proportional to the strength of the wind in the upper layer,  $U_2$ . It follows that mutual rotation is favoured by vertical weak shear, strong coupling and strong vortices. If the vortices are not sufficiently close initially, they will not undergo a complete rotation.

One can determine the rotation rate by noting that the angle  $\theta$  subtended by the upper vortex relative to the lower one is given by  $\tan\theta = Y/X$ . Differentiating this expression with respect to  $t$  and using Eqs. (6),(7),(8) and (11) gives

$$\frac{d\theta}{dt} = \frac{A}{c}(1 - \mu Y)e^{2\mu Y} \quad (12)$$

It follows that for  $\mu Y \ll 1$ , the rotation period is approximately constant, equal to  $2\pi c/A$  and that it decreases as  $\mu Y$  increases.

As explained earlier, the foregoing analogue model is conceived as an aid to understanding aspects of the interaction between a tilted vortex and a vertical shear flow. We emphasize again that the coupled pair of singular barotropic vortices does not constitute a complete model for the two-layer system and at this stage the model cannot represent the case where the vortices are initially co-located, corresponding to the situation in which a vortex with continuous vertical structure has no initial vertical tilt. In the next section we present some solutions for the case of distributed (i.e. non-singular) vortices where the vortices are initially co-located. Then, in section 4, we show that a similar, but more complete theory can be worked out for a quasi-geostrophic system where it provides a useful first approximation to numerical solutions of the full equations.

### 3. DISTRIBUTED VORTICES

It is possible to carry out calculations similar to those in sections 2 for non-singular vortices with a continuous vorticity distribution. Then Eqs. (1) and (2) must be modified by replacing  $\Gamma_n/r$  by  $v_n(r)$ , the tangential velocity of vortex- $n$  at radius  $r$ . If  $v_n(0) = 0$ , calculations of the resulting ordinary differential equations, analogous to (6) and (7), can be carried out with the vortices in each layer initially co-located. As before we assume that the distortion of the relative vorticity field of one vortex by the velocity field of the other can be neglected in as much as the evolving flow asymmetry makes a negligible contribution to the motion of that vortex. The assumption is shown to be valid in the

case of quasi-geostrophic vortices studied later in section 4, although it may not always be justified (e.g. Jones, 1999a).

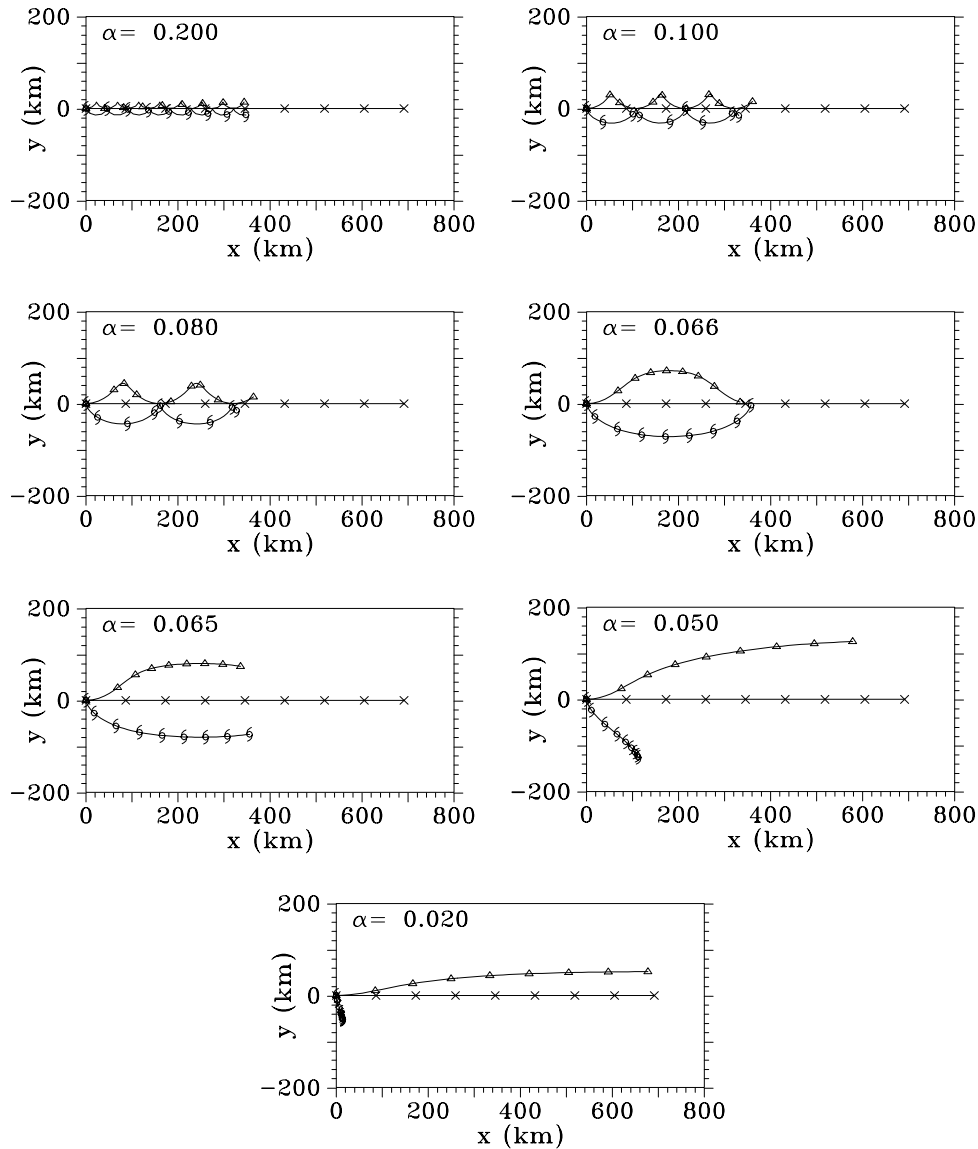


Figure 3. Trajectories of the upper and lower vortex centres for a pair of distributed vortices of equal strength that are initially co-located. The track of the upper vortex is marked by 'Δ' symbols every 6 h; the lower vortex by a cyclone symbol. Symbols 'x' mark six hourly positions of a point that is purely advected by the upper flow with speed  $U_2$ .

Figure 3 shows the tracks of the upper and lower vortices in runs where the profiles of  $v_n(r)$  are both chosen to be the same as the vortex studied by Smith *et al.* (1990) with the tangential wind speed increasing from zero at the centre to a maximum of

$v_m = 40ms^{-1}$  at a radius  $r_m$  of 100 km and a speed of  $15ms^{-1}$  at a radius of 300 km. The profile for these values has the functional form  $v(s) = v_m sa(1 + 3b^2cs^4)/(1 + bs^2 + b^3cs^6)^2$  where  $s = r/r_m$  and  $a, b, c$  are constants (here  $a = 1.7880, b = 0.3398, c = 0.0137$ ). The magnitude of  $U_2$  is  $4ms^{-1}$  and tracks are for various values of the coupling parameter  $\alpha$ . When the coupling is strong, i.e. for relatively large values of  $\alpha$ , the vortices rotate rapidly around each other as their mean position translates at the same speed as predicted by Eq. (8). This can be seen by comparing the tracks with that of a hypothetical air parcel that translates with the speed  $U_2$ , shown also in Fig. 3. As the coupling strength is reduced holding other quantities fixed, the period of mutual rotation decreases until a value of  $\alpha$  is reached for which the vortices separate, as in the case of singular vortices.

One can carry out a similar phase-space analysis to that in section 2, but the analysis must be carried out numerically. The results of such a calculation are displayed in Fig. 4, where again the abscissa and ordinate have been scaled so that the critical point  $(0, y_c)$

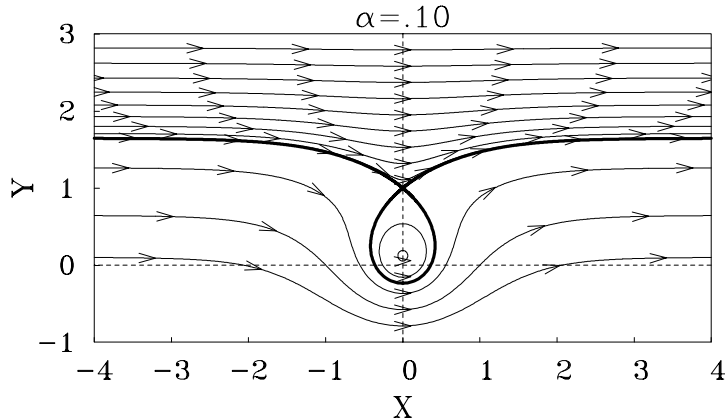


Figure 4. Legend as for Fig. 2, except for the distributed vortex calculation described in section 3. The arrows indicate the distance travelled by the upper vortex relative to the lower one during a fixed time interval.

of the differential equations (analogous to Eqs. 6 and 7) lies on the ordinate at  $Y = 1$  to facilitate comparison with Fig. 2. Figure 4 is similar in structure to Fig. 2, but the more rapid radial decay of the vortex in this case (the tangential wind speed falls off like  $(radius)^{-7}$ , compared with  $(radius)^{-1}$  for the line vortex in section 2) means that the range of influence of the two vortices is smaller and the relative trajectories outside the critical curve are more zonal in Fig. 4 than in Fig. 2.

The region where closed loops occur has a leaf-like shape that is typical for a broad range of parameters. The area of this region increases with the coupling parameter  $\alpha$ . A critical point  $(0, y_c)$  exists if  $2\alpha v(0, y_c) = U_2$  has a solution. If  $2\alpha v_m \leq U_2$ , i.e. if the coupling is too weak or the shear is too strong, no region of closed loops occurs. The width of the region of closed loops in the x-direction is found to be proportional to the vortex strength and  $\alpha/U_2$ . The upper vortex passes the lower one faster south of the critical line than to the north of it.

The behaviour of the two vortices is reminiscent of that in other calculations, such as those in the studies referred to in section 1. For example, Jones (1995, p826) notes that at the mid-level in her model, the speed of vortex motion is close to that of the speed of

the environmental flow. This is equivalent to the finding here if one identifies the mean position of the upper and lower vortex centres in the analogue model with the mid-level centre in her model. She notes also that the vertical tilt of the vortex increases with time, but is much smaller than that which would be implied by simple advection by the basic flow. Again, the analogue model shows clearly why this is the case. Except when the upper vortex is due east or due west of the lower one, one vortex is always opposing the eastward motion of the other. In this way the zonal flow in one layer is shared between the two vortices (see (5)) so that their relative eastward motion is less than if one vortex were stationary and the other simply advected by the zonal flow \*. Jones does not show a case where mutual rotation occurs without continued separation, which the analogue theory would predict for weak enough shear and/or a strong enough vortex and vertical coupling. The existence of this regime may be significant, however, and may explain why tropical cyclones frequently exhibit small-scale track oscillations. Our calculations suggest that such oscillations may be a result of the storm being subjected to weak vertical shear. The question remains, of course, to what extent one can really neglect the flow asymmetries that arise as a result of the deformation of each vortex by the flow field of the other, and the effects of divergence? Recently, Jones (1999a) has investigated the evolution of these asymmetries and has shown situations where they can have an important effect on the vortex motion. We explore this problem here on the basis of quasi-geostrophic theory and show cases where the asymmetries are much less important for the vortex motion than the mutual rotation.

#### 4. QUASI-GEOSTROPHIC MODEL

We examine now the degree to which the subsequent motion of a two-layer quasi-geostrophic vortex can be characterized by the dynamics contained in the analogue model of sections 2 and 3. In other words, to what extent can we interpret the motion of each component vortex (one in each layer) in terms of advection by the vector sum of the basic flow in its own layer and the flow associated with the *axisymmetric* circulation induced by the other vortex at its centre? The point of considering quasi-geostrophic vortices is because the two-layer quasi-geostrophic problem can be solved numerically and the invertibility relationship between the PV and the streamfunction is linear. The latter property enables us to uniquely identify the streamfunction contribution from each component vortex and to assess the errors in neglecting the flow asymmetries arising from the deformation of each vortex.

##### (a) Model formulation

For simplicity we assume that the two model layers have equal thickness  $D$ . Following Pedlosky (1987), the flow evolution is governed by the quasi-geostrophic potential vorticity equation in each layer:

$$\frac{\partial q_n}{\partial t} + J(\psi_n, q_n) = 0, \quad (n = 1, 2) \quad (13)$$

where

$$q_n = \nabla^2 \psi_n + (-1)^n \lambda^{-2} (\psi_1 - \psi_2) + \beta_n y, \quad (14)$$

\* Jones' formulation considers easterly zonal shear with zero basic flow at the upper boundary and westerly flow at the surface.

$\psi_n$  is the geostrophic streamfunction in layer- $n$ ,  $q_n$  is the pseudo-potential vorticity (PV) in that layer,  $\lambda = ND/f$  is the deformation radius,  $f$  is the Coriolis parameter and  $\beta_n = \beta + \mu_n$ , where  $\beta = df/dy$  and  $\mu_n$  is a constant to be defined below. We separate  $q_n$  and  $\psi_n$  into a basic state contribution which depends only on  $y$  and is denoted by an overbar, and a vortex part, denoted by a prime. Then

$$\bar{q}_n = \frac{d^2 \bar{\psi}_n}{dy^2} + (-1)^n \lambda^{-2} (\bar{\psi}_1 - \bar{\psi}_2) + \beta_n y, \quad (15)$$

$$q'_n = \nabla^2 \psi'_n + (-1)^n \lambda^{-2} (\psi'_1 - \psi'_2), \quad (16)$$

and  $q'_n$  satisfies

$$\left( \frac{\partial}{\partial t} + \bar{u}_n \frac{\partial}{\partial x} \right) q'_n + J(\psi'_n, \bar{q}_n) + J(\psi'_n, q'_n) = 0, \quad (17)$$

where  $\bar{u}_n = - (d\bar{\psi}_n/dy)$ . The basic state potential vorticity gradient in each layer is obtained by differentiating Equation (15), i. e.,

$$\frac{\partial \bar{q}_n}{\partial y} = (-1)^n \lambda^{-2} (U_2 - U_1) + \mu_n. \quad (18)$$

Note that  $J(\psi'_n, q'_n) = k \cdot \nabla \psi'_n \wedge \nabla q'_n$ . Moreover, for a symmetric vortex, both  $\nabla \psi'_n$  and  $\nabla q'_n$  lie in the radial direction, whereupon  $J(\psi'_n, q'_n) = 0$ . However, an initially-symmetric vortex will remain symmetric only if  $J(\psi'_n, \bar{q}_n) = 0$  and only if there is no mean vertical shear (i.e.  $\bar{u}_1 = \bar{u}_2$ ). The former condition is satisfied only if the basic state potential vorticity gradient is zero, which we assume to be the case. The requirements are that  $\beta = 0$  and  $\mu_n = (-1)^n \lambda^{-2} (U_1 - U_2)$ , i.e. the upper and lower boundaries of the domain slope linearly in the  $y$ -direction, parallel to the internal fluid interface, with slope  $\mu_n y \lambda / N$ . The quasi-geostrophic equations are restricted by the requirement that the Rossby-number  $Ro = U/(fL)$  is small compared with unity. In particular, the size of  $Ro$  affects the interface displacement  $Ro \lambda^{-2} (\psi_2 - \psi_1)$ . If  $Ro$  is too large, negative layer thicknesses may result in the model if the shear and/or coupling rates are large and if the domain extends far in the  $y$ -direction.

One limitation of the analogue model is that it does not allow the interface between the upper and lower vortices to deform. This restriction can be removed in the quasi-geostrophic model.

We consider first an initially-symmetric cyclonic vortex centred at the point  $\mathbf{r}_2$  in which the PV-distribution is confined to the upper layer; i.e. let  $q_2(\mathbf{r}; t) = Q_2(|\mathbf{r} - \mathbf{r}_2|)$  and  $q_1(\mathbf{r}; t) \equiv 0$ , where here,  $\mathbf{r} = (x, y)$  and  $\mathbf{r}_2 = (x_2, y_2)$ . The corresponding streamfunction in each layer can be obtained by solving the invertibility relation represented by Eq. (16). When this is done, the relative vorticity in the lower layer is simply  $\lambda^{-2} (\psi'_2 - \psi'_1)$ . Suppose now that the upper-level PV-distribution is advected zonally by the differential shear illustrated in Fig. 1. As explained, for example, by Hoskins et al. (1985, section 4), the associated low-level disturbance must translate with it. However, as there is no zonal flow in the lower layer, this is possible only by the process of development as envisaged by Sutcliffe (1947); i.e. in layer-1 there must be stretching of planetary vorticity through ascent of the interface to the east of the upper-level PV-distribution and contraction of planetary vorticity to the west. In other words, an azimuthal wavenumber-one pattern of divergence is necessary for the translation of the associated (zero-PV) vortex in the lower layer and this destroys the initial symmetry of the flow, leading to a wavenumber-one pattern of relative-vorticity tendency. The effect is clearly not captured by the theory developed in section 2 and, to the extent that it is important for the subsequent vortex

motion, its omission places a limitation on that theory.

The possibility arises of refining the theory of sections 2 and 3, at least for the quasi-geostrophic case, by considering the interaction of *singular* upper and lower PV-anomalies in the two-layer flow. The structure of these is given by Gryanik (1983) and Hogg and Stommel (1985). However, since such disturbances are associated with relative vorticity distributions that are not confined to a point, it seems just as profitable here to examine the case of distributed vortices from the outset. Accordingly, we consider now an initial vortex in the two-layer model to be made up of a pair of PV-distributions and their associated flow fields as described above, one in each layer. We refer to the two component vortices as vortex-1 and vortex-2. Vortex-1 has a PV-distribution  $q_1$  confined entirely to the lower layer and vortex-2 has a PV-distribution  $q_2$  confined entirely to the upper layer. The flow associated with each PV-distribution has a relatively strong contribution in its own layer and a weaker one in the other layer. The geostrophic streamfunction of the vortex in layer-1,  $\psi_L$ , is the sum of the streamfunction contribution from the PV-distribution in that layer,  $\psi_{L1}$ , and from the streamfunction contribution from the PV-distribution in layer-2,  $\psi_{L2}$ . Likewise, the geostrophic streamfunction of the vortex in layer-2,  $\psi_U$ , is the sum of the streamfunction contribution from the PV-distribution in that layer,  $\psi_{U2}$ , and from the streamfunction contribution from the PV-distribution in layer-1,  $\psi_{U1}$ . At the initial time, the streamfunction pairs  $(\psi_{L1}, \psi_{L2})$  and  $(\psi_{U1}, \psi_{U2})$  satisfy the steady axisymmetric quasi-geostrophic equations:

$$\begin{pmatrix} L - \lambda^{-2} & \lambda^{-2} \\ -\lambda^{-2} & L + \lambda^{-2} \end{pmatrix} \begin{pmatrix} \psi_{L2} & \psi_{U2} \\ \psi_{L1} & \psi_{U1} \end{pmatrix} = \begin{pmatrix} 0 & q_2 \\ q_1 & 0 \end{pmatrix} \quad (19)$$

where  $L \equiv d^2/dr^2 + r^{-1}d/dr$  and  $r$  is the radius. The inverse of the constant  $\lambda$  is a measure of the strength of coupling between the two vortices, equivalent to the coupling coefficient  $\alpha$  in sections 2 and 3. Note that a potential vorticity anomaly with horizontal scale  $L$  in a continuously stratified fluid has a penetration depth scale  $H_R = fL/N$ , where  $N$  is the Brunt-Vaisala frequency. In the two-layer fluid considered here, the quantity  $g\Delta\rho/(H\rho)$  plays the role of  $N$ , where  $\Delta\rho$  is the density contrast between the layers. Then the influence of an anomaly in the upper layer on the flow in the lower layer decreases as the scale of the anomaly decreases or as  $\Delta\rho$  increases. At later times, when the vortices have become non-axisymmetric, the PV-distribution in each layer is radially-averaged about the vortex centre in that layer to obtain new symmetric distributions of PV: say  $\tilde{q}_1$  and  $\tilde{q}_2$ . The vortex centre in a layer is defined as the location of the maximum PV in that layer. With these new profiles of  $q_n$ , the two columns of Eq. (19) are solved separately for the symmetric streamfunctions for vortex-1 and vortex-2. We may then calculate the flow speed and direction at the centre of each vortex associated with the symmetric circulation of the other vortex. The extent to which this flow characterizes the motion of the two vortices in a full numerical solution of the quasi-geostrophic problem is a measure of the applicability of the analogue model in this case.

(b) *Results*

The full quasi-geostrophic model is initialized with a barotropic vortex having the same profile of tangential wind speed as in section 3, but with  $r_m = 500km$  and  $v_m = 10ms^{-1}$ . For a mid-latitude value of  $f (= 10^{-4}s^{-1})$ , the vortex Rossby number,  $Ro = v_m/(fr_m)$ , has the value 0.24. The nondimensional Rossby radius of deformation,  $\lambda/r_m = 1.67$ . A zonal flow  $U_2 = 2ms^{-1}$  is applied in the upper layer whereas there is no background flow in the lower layer. As a result, the vortex begins to tilt and the location of

the upper and lower vortex centres separate. The tracks of the two component vortices in this calculation are displayed in Fig. 5. As in the analogue model, the vortices loop

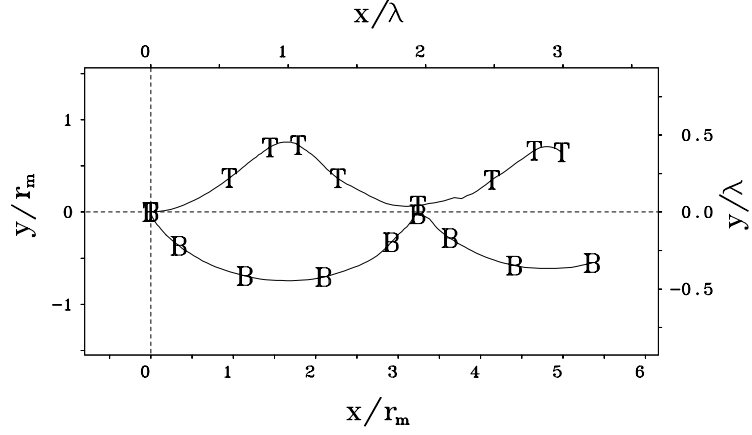


Figure 5. Trajectories of the upper and lower vortex centres for a pair of distributed vortices of equal strength that are initially co-located. The track of the upper vortex is denoted by 'T' every 6 h (about 6.5 time units,  $r_m/v_m$ ) and the lower vortex by 'B'. Nondimensional Rossby deformation radius  $\lambda/r_m = 1.67$ .

around a translating mean centre which moves at a speed of  $\frac{1}{2}U_2$ .

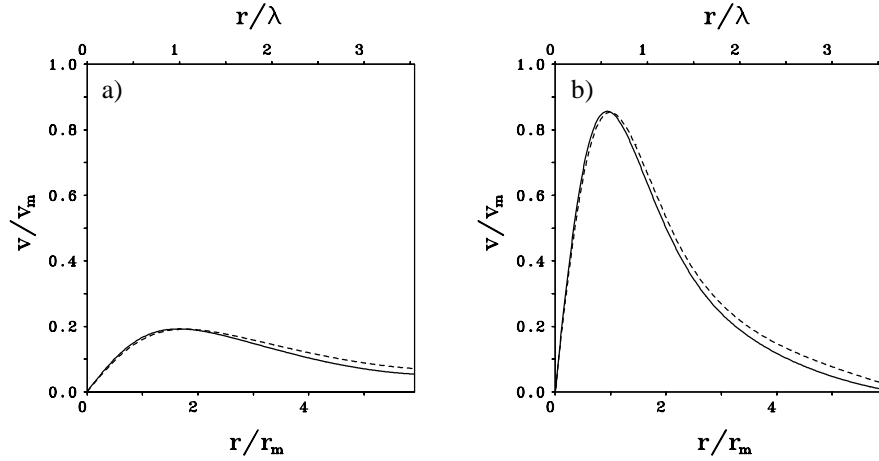


Figure 6. Radial profiles of tangential wind speed for (a) vortex-1, and (b) vortex-2, at an early time (0.4 time units, solid) and a later time (26 time units, dashed). Time unit is  $r_m/v_m$ .

Figure 6 shows the radial profiles of tangential wind speed for vortex-1 at an early time (solid) and a later time (dashed) in dimensionless time units  $r_m/v_m$ . The profiles

are obtained by solving the first column of Eq. (19) with the radially-averaged PV-distribution on the right-hand-side. In this case the ratio of maximum tangential wind speed in the lower layer to that in the upper layer is about 4:1. Note also that the profiles do not change appreciably with time. As expected, the profiles for vortex-2 are identical, but the layers are reversed.

Figure 7a compares the translation speed components,  $U$  and  $V$ , of the upper vortex with the velocity components of the symmetric flow across its centre associated with the lower vortex (the corresponding dashed curves) as a function of time. Similar comparisons are shown in Fig. 7b for the translation speed components of the lower vortex. The relatively good agreement of the corresponding sets of curves indicates that the dynamics represented by the analogue model of section 3 captures the essence of the flow evolution in this case. However, it is not possible to provide a full comparison of the two theories because, in the quasi-geostrophic case, the tangential velocity profile of the upper part of each component vortex is not a constant multiple of the profile of the lower part. This is exemplified by the singular vortex solutions given by Gryanik (1983) and Hogg and Stommel (1985).

The two panels in Fig. 7 show also the velocity components at the centre of each vortex when the flow components associated with the asymmetric PV-distribution in the other layer are added to the corresponding  $U$  and  $V$  curves (the dotted curves). These curves lie very close to those for the translation speed of each vortex, confirming that the symmetric and asymmetric components together account for all of the motion. Thus the difference between the  $U$  or  $V$  curve and the corresponding component of translation velocity is a measure for the asymmetric flow across the centre of the two vortices.

Figures 8-10 show diagrams similar to Figs. 5-7, but for a calculation in which the Rossby deformation radius  $\lambda$  is larger than  $r_m$ . For this case the coupling between layers is weaker or equivalently the penetration depth is smaller, and the vortices separate (Fig. 8). As in the previous case, the profiles of mean tangential wind speed do not vary appreciably with time, but in this case the ratio of maximum tangential wind speed in the lower layer to that in the upper layer is about 9:1 (Fig. 9). In this case also, the relatively good agreement of the corresponding sets of curves indicates that the dynamics represented by the analogue model of section 3 captures the essence of the flow evolution.

One cannot construct a phase-space diagram for the full geostrophic solutions, because the vortices become distorted and the subsequent flow evolution depends not only on the positions of the vortices at the current time, but also on the history of the flow. However, one can construct diagrams such as Fig. 11 which shows whether looping motion, possibly with alignment, or separation will occur as a function of the relative positions of the upper and lower vortices. Vortex alignment is the stratified counterpart of vortex merger in a barotropic fluid system and refers to a mean decrease in the horizontal distance between the upper and lower vortex centres on a time scale long compared with the period of looping motion about the mean centre (Polvani, 1991).

As in Figs. 2 and 4, the lower vortex is located at the origin. For initial positions of the upper vortex denoted by a cyclone symbol, the vortices execute looping motions and eventually align. For initial positions denoted by a downward-pointing arrow, the upper vortex passes to the south of the lower vortex and then on to the east. For initial positions marked by a star, the upper vortex moves with an eastward component away from the lower vortex. The critical curve which divides looping motions and alignment from separation is again leaf-shaped, but the axis is inclined towards the northwest. A detailed analysis of the alignment process is beyond the scope of the current work, but it is worth noting that the approach of the two vortex centres is not monotonic during the merger.

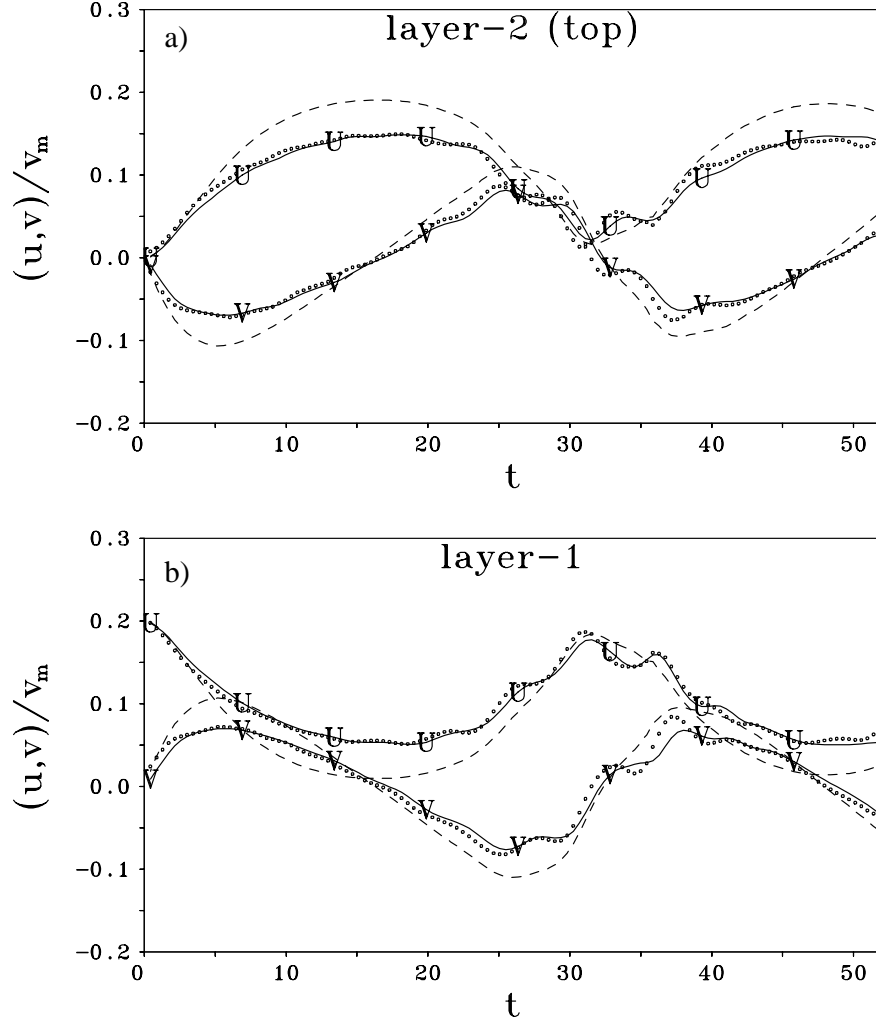


Figure 7. Comparison between the translation speed components,  $U$  and  $V$ , of (a) the upper vortex, and (b) the lower vortex, and the velocity components of the symmetric flow of the other vortex across its centre (the corresponding dashed curves) as a function of nondimensional time (time unit  $r_m/v_m$ ). The dotted curves in each panel show the velocity components at the centre of each vortex when the flow components in its layer associated with the asymmetric PV-distribution of the other vortex are added to the corresponding dashed curves.

## 5. DISCUSSION

It is of interest to contrast the present study with that of vortex alignment in a two-layer quasi-geostrophic model by Polvani (1991) and with the study of singular two-layer quasi-geostrophic vortices on a beta-plane by Reznik et al. (1997). Polvani investigates the interaction of initially-circular vortex patches (vortices consisting of finite regions

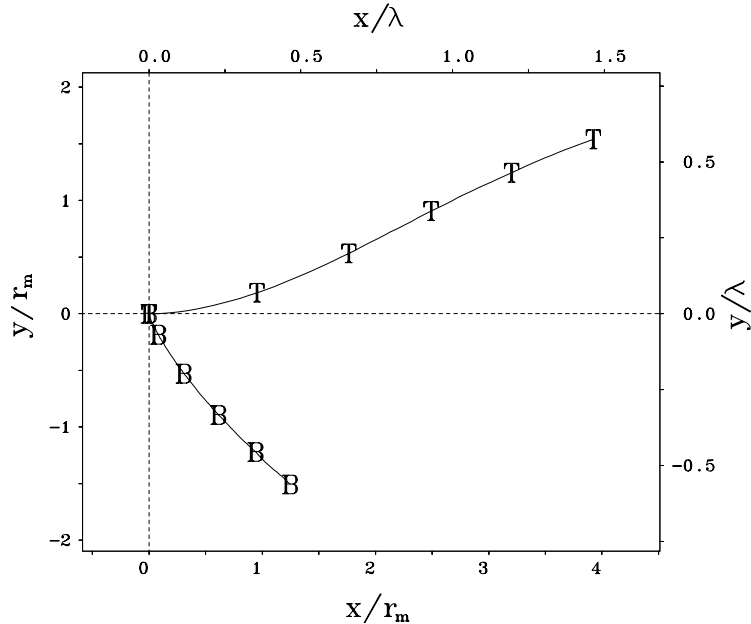


Figure 8. Legend as for Fig. 5, except for  $\lambda/r_m = 2.68$ , Symbols all 5.18 time units.

of uniform potential vorticity), one in each layer, but does not consider the effects of vertical shear. He shows that alignment depends on the initial vortex separation and Rossby radius of deformation compared to the vortex size. Our analogue model would always predict the mutual rotation of the two vortices in the absence of vertical shear, since the critical point  $(0, y_c)$  tends to infinity as  $U_2$  tends to zero.

Reznik et al. (1997) present an analytic theory of purely baroclinic two-layer singular vortices on a beta-plane and identified four mechanisms governing the vortex motion. These are (i) barotropic beta-gyres, (ii) baroclinic beta gyres, (iii) the interaction between the lower-layer and upper-layer vortices, and (iv) Rossby-wave radiation. Like Polvani op. cit. they do not consider vertical shear, but calculations by other authors indicate the importance of the beta-gyre asymmetries in addition to those induced by vertical shear (see e.g. Shapiro, 1992; Flatau *et al.*, 1994; and Wang and Holland, 1996).

The situation in tropical cyclones is likely to be much more complicated than in the calculations described in this paper and those referred to above. For one thing, the quasi-geostrophic assumption is invalid, at least on the scale of the vortex core, and there are typically two independent scales characterizing the vortex: the radius of maximum tangential wind speed and the radius of gale-force winds. The latter characterizes the rate of radial decay of the tangential wind field. The additional scale may produce a even richer range of behaviour than that in the quasi-geostrophic calculations of Polvani op. cit..

A further complication, discussed by Jones (1995), is that at Rossby numbers that are not small compared with unity, the Rossby radius of deformation is a function of radius, inversely proportional to the inertial stability. This means that the penetration depth

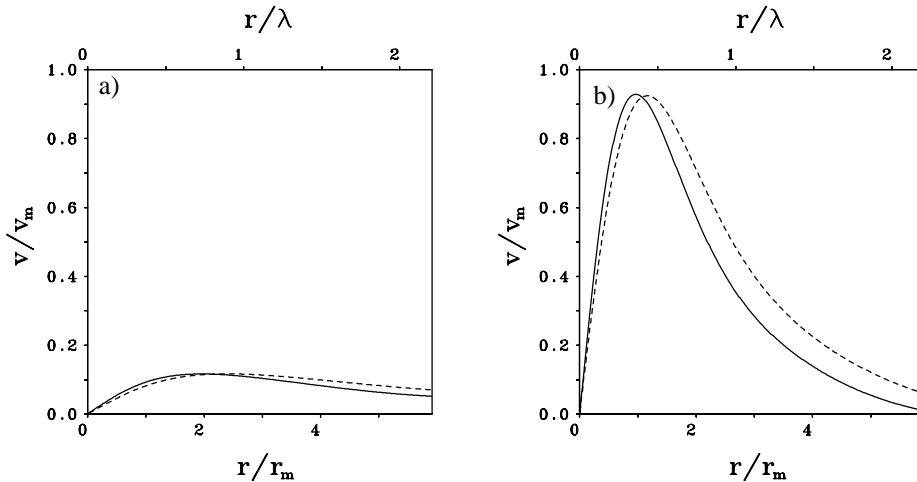


Figure 9. Legend as for Fig. 6, except after 17.8 time units and for  $\lambda/r_m = 2.68$ .

varies with radius also. Some as yet unpublished comparisons we have made between the predictions of quasi-geostrophic theory and those using the primitive equations show that the former theory underestimates the penetration depth for strong vortices with Rossby numbers comparable with or greater than unity. In other words, the strong vortices are more able to resist the effect of vertical shear.

Finally, it is likely that vertical coupling by convective momentum transport plays an important role also in the behaviour of vertically-sheared storms (see e.g Shapiro, 1992; Dengler and Reeder, 1996). Despite these additional complications, the mechanisms represented in the analogue model go a long way to understanding the range of behaviour in the calculations by Jones and others and it is reasonable to presume that they are fundamental in tropical cyclones also.

## 6. CONCLUSIONS

We have presented solutions for a simple two-layer analogue model in order to elucidate some aspects of the dynamics of vortex motion in vertical shear. The model is based on the idea that the motion of the vortex in each layer can be approximated by the symmetric flow of the other vortex at its centre, together with any basic flow in that layer. We show that the assumption provides a good first approximation for interpreting the motion of quasi-geostrophic vortices in vertical shear. The calculations indicate two types of flow behaviour according to the strength of the two component vortices, the degree of vertical coupling and the strength of the shear. If the component vortices are strong, the vertical coupling is strong and the shear is weak, the vortices rotate around each other as their mean centre translates with a fraction of the zonal flow speed. The fraction is the ratio of the circulation strength of the upper vortex to the sum of the circulation strengths of both vortices. If the component vortices are weak, the vertical coupling is weak and the shear is strong, the vortices become progressively separated by

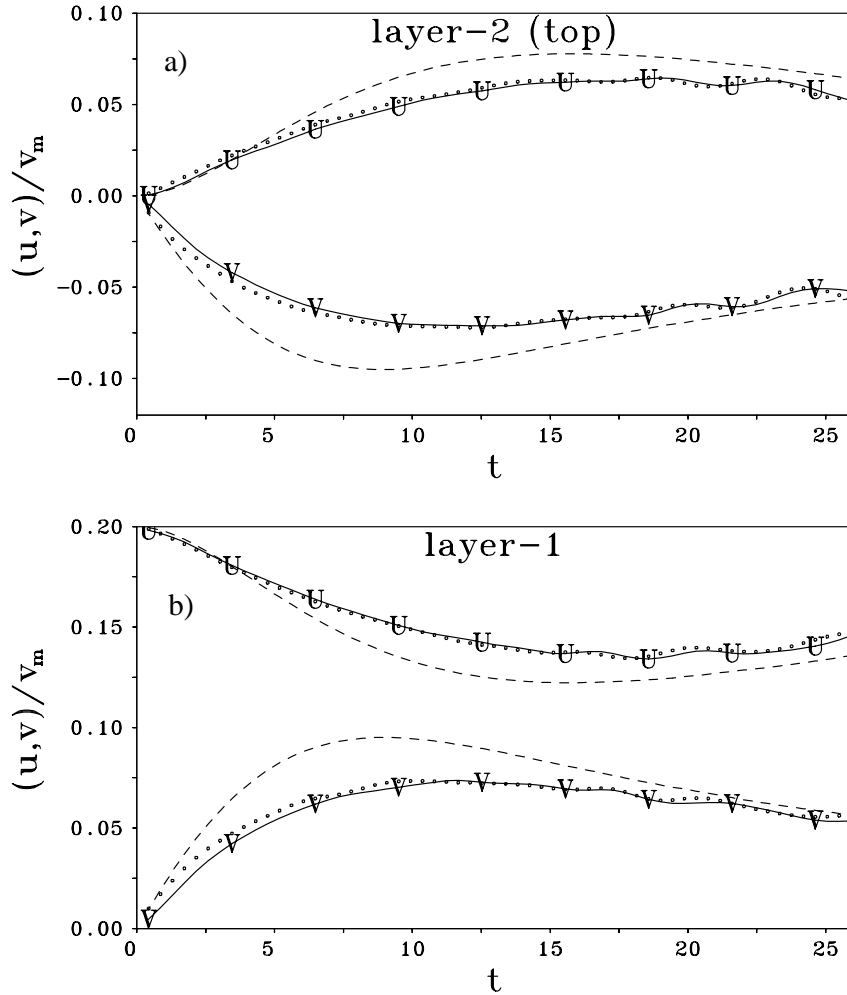


Figure 10. Legend as for Fig. 7, except for  $\lambda/r_m = 2.68$ .

the shear while undergoing a partial rotation about each other while they are still close.

We suggest that the processes isolated in the analogue model are likely to be of fundamental importance in understanding the behaviour of tropical cyclones in vertical shear. Indeed the prediction that strong vortices exposed to weak vertical shear undergo mutual rotation as they propagate provides a possible explanation for the small-scale track oscillations of tropical cyclones that are frequently observed.

ACKNOWLEDGEMENTS

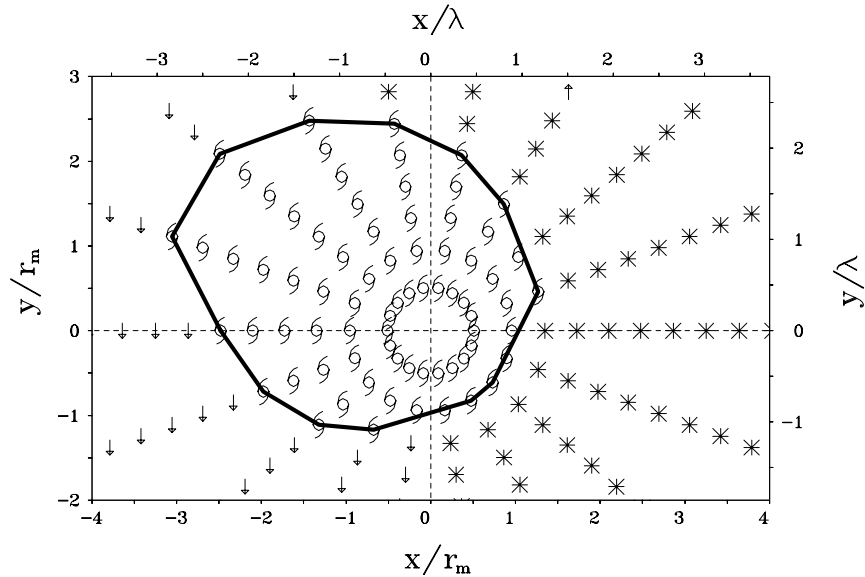


Figure 11. Track regimes for the upper vortex as a function its initial location relative to the lower one. At points marked by a cyclone symbol, the upper vortex loops around the lower one and in some cases converges towards it (i.e. the vortices align). The solid contour encloses the region where looping or converging motion occurs. At points marked by a downward-pointing arrow, the upper vortex first moves towards and cyclonically around the lower vortex and then continues on to the right. At points marked by a star, the upper vortex separates from the lower vortex, moving to the right.

We are very grateful to Sarah Jones and an anonymous reviewer for their perceptive comments on an earlier version of this manuscript. The work was supported by the US Office of Naval Research through Grant No. N00014-95-1-0394.

#### REFERENCES

- |   |      |  |
|---|------|--|
| Dengler, K. and M. J. Reeder                    | 1996 | The effects of convection and baroclinicity on the motion of tropical-cyclone-like vortices. <i>Quart. J. Roy. Meteor. Soc.</i> , <b>123</b> , 699-727                                     |
| Flatau, M., W.H. Schubert and D.E. Stevens      | 1994 | The role of baroclinic processes in baroclinic vortex motion. The influence of vertical tilt. <i>J. Atmos. Sci.</i> , <b>51</b> , 2589-2601  |
| Gryanik, V. M.                                  | 1983 | Dynamics of singular geostrophic vortices in a two-level model of the atmosphere (or ocean). <i>Izvestia Atmos. Ocean Phys.</i> , <b>19</b> , 171-179                                      |
| Hogg, N.G., and H. M. Stommel                   | 1985 | The heton, an elementary interaction between discrete baroclinic geostrophic vortices, and its implications concerning eddy heat flow. <i>Proc. Roy. Soc. Lond. A.</i> , <b>397</b> , 1-20 |
| Hoskins, B.J., M.E. McIntyre and A.W. Robertson | 1985 | On the use and significance of isentropic potential vorticity maps. <i>Quart. J. Roy. Met. Soc.</i> , <b>111</b> , 877-946   |
| Jones, S.C.                                     | 1995 | The evolution of vortices in vertical shear: I: Initially barotropic vortices. <i>Quart. J. Roy. Met. Soc.</i> , <b>121</b> , 821-851  |

- Jones, S.C. 2000a The evolution of vortices in vertical shear: II: the role of large-scale asymmetries. *Quart. J. Roy. Met. Soc.*, (in press)
- Jones, S.C. 2000b The evolution of vortices in vertical shear: III: Baroclinic vortices. *Quart. J. Roy. Met. Soc.*, (in press)
- Madala, R. V., and Piacsek, S. A. 1975 Numerical simulation of asymmetric hurricanes on a beta-plane with vertical shear. *Tellus.*, **27**, 453-468
- Pedlosky, J. 1987 Geophysical Fluid Dynamics. Springer, New York, 416-424
- Polvani, L.M. 1991 Two-layer geostrophic vortex dynamics. Part 2. Alignment and two-layer V- states. *J.Fluid. Mech.*, **225**, 241-270
- Reznik, G.M. and W.K. Dewar 1994 An analytic theory of distributed barotropic axisymmetric vortices on the b-plane. *J. Fluid Mech.*, **269**, 301-321
- Reznik, G.M. R.H.J. Grimshaw and K. Sriskandarajah 1997 On basic mechanisms governing the evolution of two-layer localized quasi-geostrophic vortices on a b-plane. *Geophys. Astro. Fluid Dyn.*, **86**, 1-42
- Shapiro, L. J. 1992 Hurricane vortex motion and evolution in a three-layer model. *J. Atmos. Sci.*, **49**, 140-153
- Shapiro, L. J., and Montgomery, M. T. 1993 A three-dimensional balance theory for rapidly rotating vortices. *J. Atmos. Sci.*, **50**, 3322-3335
- Smith, R.K., 1993 On the theory of tropical cyclone motion. In. *Tropical Cyclone Disasters.*, Ed. Lighthill et al., Peking University Press, Beijing, 264-279.
- Smith, R.K., Ulrich, W., and Dietachmayer, G. 1990 A numerical study of tropical cyclone motion using a barotropic model I: the role of vortex asymmetries. *Q.J.R.Meteorol.Soc.*, **116**, 337-362
- Sutcliffe, R. 1947 A contribution to the problem of development. *Quart. J. Roy. Met. Soc.*, **73**, 370-383
- Wu, C-C and Emanuel K.A. 1993 Interaction of a baroclinic vortex with background shear: Application to hurricane movement. *J. Atmos. Sci.*, **50**, 62-76
- Wang, B., and Li, X. 1992 The beta drift of three-dimensional vortices: a numerical study. *Mon. Wea. Rev.*, **120**, 579-593
- Wang, Y., and Holland, G. J. 1996 Tropical cyclone motion and evolution in vertical shear. *J. Atmos. Sci.*, **53**, 3313-3332
- Wang, Y., Holland, G. J. and Leslie, L. M. 1993 Some baroclinic aspects of tropical cyclone motion. Pp.280-285 in *Tropical Cyclone Disasters.*, Eds. J. Lighthill, K. Emanuel, G. Holland and Z. Zhemmin. Peking University.